Mol. Cells *35*, 436-443, May 31, 2013
DOI/10.1007/s10059-013-0046-5
eISSN: 0219-1032

Molecules and Cells
http://molcells.org
Established in 1990

The Effect of Amino Density on the Attachment, Migration, and Differentiation of Rat Neural Stem Cells *In Vitro*

Hai-Long Li, Han Zhang, Hua Huang, Zhen-Qiang Liu, Yan-Bing Li, Hao Yu, and Yi-Hua An*

Artificial extracellular matrices play important roles in the regulation of stem cell behavior. To generate materials for tissue engineering, active functional groups, such as amino, carboxyl, and hydroxyl, are often introduced to change the properties of the biomaterial surface. In this study, we chemically modified coverslips to create surfaces with different amino densities and investigated the adhesion, migration, and differentiation of neural stem cells (NSCs) under serum-free culture conditions. We observed that a higher amino density significantly promoted NSCs attachment, enhanced neuronal differentiation and promoted excitatory synapse formation *in vitro*. These results indicate that the amino density significantly affected the biological behavior of NSCs. Thus, the density and impact of functional groups in extracellular matrices should be considered in the research and development of materials for tissue engineering.

INTRODUCTION

The use of neural stem cells (NSCs) in tissue engineering is a promising treatment for central (Bible et al., 2009; Hwang et al., 2011; Johnson et al., 2010; Olson et al., 2009) and peripheral nervous system damage (Zhang et al., 2008). Cell adhesion, migration, and differentiation are highly dependent on the surrounding microenvironment, particularly the physical and chemical surface properties of biological materials. In some cases, engineered materials can affect adsorption of cells and induce biological responses (Keselowsky et al., 2004). A number of active fragments, including peptide chains, poly-amino acids, or active chemical functional groups, have been introduced onto the surfaces of biological materials (Ananthanarayanan et al., 2010; Cook et al., 1997; Teng et al., 2007). These fragments contain functional groups, such as amino, carboxyl, and hydroxyl, that facilitate cell attachment and growth (Lee et al., 1994; Li et al., 2005).

Attachment is an important prerequisite for NSCs growth, migration and differentiation. Previously, we confirmed that functional groups differentially affect the behavior of NSCs. Compared with other chemically active groups, amino significantly promotes the adhesion and migration of NSCs on chemically modified coverslips and enhances neuronal differentiation (Ren et al., 2009). Since poly-lysine coated dishes were commonly used to culture NSCs (Wang et al., 2006), we reason that the amino functional group, which has positive charge characteristics and best affinity, might be the most suitable for cell adhesion because the cell surface is negatively charged. Although hydrophilicity is an important factor for cell attachment, migration, and growth on polymers, other studies have demonstrated that the chemical properties and charge characteristics of biomaterial surfaces also play important roles (Horwitz et al., 2010; Lee et al., 1994; Zelzer et al., 2008). Furthermore, media containing serum (Vasita et al., 2008) or attachment proteins (Brewer and Torricelli, 2007; Ho et al., 2006; Keselowsky et al., 2004) in experimental methods influence cell attachment and may obscure the contribution of surface chemical groups to cell behavior. Accordingly, we excluded these factors from our study.

The transmission of information between cells influences cell development and cell biology (Badoyannis et al., 1991; Li et al., 2005; Symons et al., 2002). Therefore, the density of NCSs that adhere to and grow along the surface of a substrate might affect their potential to migrate and differentiate. Since amino groups likely participate in cell attachment, altering the density of amino on the surface of the substrate might affect the density of NSCs. In this study, we designed a chemical modification method to obtain coverslips with different amino densities. The NSCs were plated on the modified material and cultured in medium without serum or attachment molecules to elucidate the effect of amino density on attachment, migration, and differentiation and characterize the mechanisms underlying these effects.

MATERIALS AND METHODS

Preparation of coverslips with different amino densities

Clean coverslips (10 mm diameter; glass; Jijin Chemistry and Technology Co. Ltd., China) were soaked in concentrated sulfuric acid and 30% hydrogen peroxide solution for hydroxylation,

Beijing Neurosurgical Institute, Beijing Tiantan Hospital, Capital Medical University, Beijing 100050, China
*Correspondence: sjwkyjs@gmail.com

Received February 8, 2013; revised March 18, 2013; accepted March 20, 2013; published online April 29, 2013

Keywords: biocompatible, cell adhesion molecular, cell migration assays, coated materials, neural stem cells

Springer

and treated with 3-aminopropyl-triethoxysilane (Sigma Chemical Co., USA) for amino addition. The reaction time, temperature, and 3-aminopropyl-triethoxysilane density were regulated to generate different amino densities on the surfaces of coverslips.

Material surface characterization

The surface properties of the modified coverslips were analyzed using the water contact angle (WCA) measurement, attenuated total reflection Fourier transform infrared spectroscopy (ATR-FTIR), and X-ray photoelectron spectroscopy (XPS). An OCA15+ optical contact angle-measuring instrument (Data Physics, Germany) was used to measure the water contact angles. A Tensor 27 infrared spectrometer (Bruker, Germany) in attenuated total reflection mode was used for the semi-quantitative detection of the relative density of amino on the material surface. The qualitative detection of amino groups on the modified matrix was performed using a PHI Quant era SXM Scanning X-ray Photoelectron Spectroscopy Microprobe ULVAC (PHI INC., Japan).

Quantitative determination of amino density using acid orange-7

The surface density of the amino groups on the modified substrate was determined using acid orange-7 dye (Tokyo Kaseo Kogyo Co., Ltd., Japan) as previously described (Hu et al., 2002). The surface density of the amino groups was determined spectrophometrically at 485 nm (Ultrospec 1,100 pro, Biochrom Ltd., UK).

Culturing of Rat NSCs on the surfaces

This study was carried out in strict accordance with the common international guideline entitled "Guide for the Care and Use of Laboratory Animals (Eighth Edition, Washington)". The protocol was approved by the Committee on the Ethics of Animal Experiments of Capital Medical University. The rat was bred as specified-pathogen-free (SPF) and given food and water freely. Decapitation was executed under sodium pentobarbital anesthesia. All efforts were made to minimize suffering.

Based on the detailed procedures for rat NSCs isolation and neurosphere culture (Brewer and Torricelli, 2007), NSCs were separated from the telencephalon of a 14-day fetus collected from a pregnant Sprague Dawley rat (purchased from Beijing Laboratory Animal Research Center). The cells were harvested and suspended in culture medium containing DMEM/F12, B-27 supplement, 20 ng/ml of EGF and 20 ng/ml of bFGF, then filtered with a sterile 400-mesh filter, stained with trypan blue, counted with a hemocytometer, and evaluated for cell viability. Cells were seeded at a ratio of 5×10^5 ml of medium in a 75-ml culture flask (Corning, USA) and cultured in suspension in an incubator at 37°C with 5% CO_2. The medium was half-changed every three days; neurospheres formed after three to five days and were collected by centrifugation. The supernatant was discarded. The pellet was beaten and blown again into a single-cell suspension for passaging.

Passage 2 NSCs were seeded onto amino modified coverslips for culturing and observation in serum-free medium containing DMEM, B-27 supplement, 12.5 ng/ml of EGF and 12.5 ng/ml of bFGF, simultaneously onto poly-l-lysine (PLL)-coated coverslips as a control group.

Detection of cell behavior

Double immunostaining

After culturing for seven days, the cells were double immunostained. The primary antibodies were mouse anti-Nestin monoclonal antibody (1:200; Millipore, USA), mouse anti-β-tubulin III monoclonal antibody (1:100; Millipore, USA), rabbit anti-GFAP monoclonal antibody (1:400; Epitomics, USA), and anti-O_4 monoclonal antibody (1:100; Millipore, USA). The secondary antibodies were rhodamine-labeled goat anti-rabbit antibody (1:200; Jackson Immunoresearch, USA), FITC DyLight 488-labeled goat anti-mouse antibody (1:200; Jackson Immunoresearch, USA), and FITC DyLight 488-labeled goat anti-mouse antibody (1:100; Millipore, USA). PBS (pH 7.4-7.6, 0.01 M) was used as a wash buffer. 4′,6-diamidino-2-phenylindole (DAPI, Invitrogen, USA) was used to stain the cell nuclei. PBS was used in place of primary antibodies as a negative control. Cells were observed using a fluorescence microscope (Olympus, Japan).

Quantification of the migration and subtype of the cells after NSCs differentiation

The cells migrating from the neurospheres in each group were stained with DAPI. The stained cells were counted using Image Pro-Plus software (version 6.1) (Ho et al., 2006). To quantify the cell subtypes after differentiation, DAPI-positive neurons, astrocytes, and oligodendrocytes were distinguished using antibodies against β-Tubulin III, GFAP, and O_4, respectively. The ratio of the three cell types was calculated as a percentage of the total number of DAPI-positive cells.

Cell ultrastructure observation using scanning electron microscopy (SEM) and transmission electron microscopy (TEM)

The NSCs cultured for five days on each surface were fixed, dehydrated in an ethanol gradient, sprayed with gold after drying, and observed under a scanning electron microscope (SEM LEO-1530). The NSCs cultured for seven days on an amino surface were scraped using a cell scraper, fixed, dehydrated, embedded, and sectioned into ultrathin slices. The sections were double-stained and observed under a Hitachi-7650 (Japan) transmission electron microscope.

Statistical analysis

The data are presented as the means ± standard error and analyzed using SPSS 13.0 software. One-way analysis of variance (ANOVA) was used for pairwise comparisons among multiple sample means. Tukey's post-hoc multiple comparison tests were used for inter-group comparisons. The level of statistical significance was set at $P < 0.05$.

RESULTS

Grouping amino densities based on ATR-FTIR spectroscopy and the acid orange-7 assay

Based on ATR-FTIR spectroscopy and the acid orange-7 assay, we selected four groups of coverslips with amino densities approximating ratios of 1:3:4:13, indicated as groups A, B, C, and D (Table 1), respectively. The corresponding aminosilane concentrations and reaction times used in each group were: 0.5% for 6 h (group A); 0.5% for 12 h (group B); 10% for 2 h (group C); and 10% for 12 h (group D).

Hydrophilicity measurement

The water contact angle, an indicator of hydrophilicity, increa-

Table 1. Materials surface characterization

Sample	Amino densities (μmol/mm^2)	WCA (means ± SD)	ATR-FTIR				
			Wavenumber (cm^{-1})	Peak value	Relative ratio of peak value	Peak area	Relative ratio of peak area
A(0.5% 6 h)	0.048 ± 0.006	34.8 ± 2.7	2,976	0.00081	1	0.08794	1
B(0.5% 12 h)	0.128 ± 0.014	45.1 ± 1.9	2,964	0.00272	3.35	0.25686	2.9
C(10% 2 h)	0.170 ± 0.010	61.3 ± 3.1	2,961	0.00358	4.42	0.33438	3.8
D(10% 12 h)	0.268 ± 0.013	86.2 ± 5.0	2,978	0.00972	12	1.15562	13.1

WCA, water contact angle; ATR-FTIR, attenuated total reflectance Fourier transform infrared spectroscopy

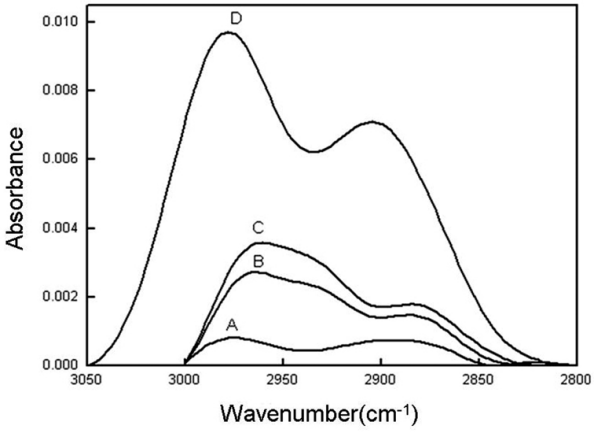

Fig. 1. Hydrocarbon peaks obtained using ATR-FTIR. (A-D) represent the different amino-density groups, as listed in Table 1. (A-D), amino modified surfaces with different densities.

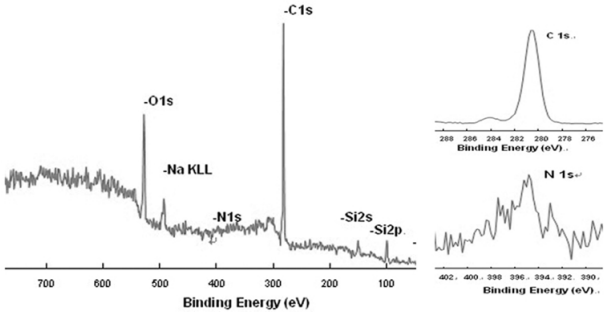

Fig. 2. A representative graph of the full XPS spectrum. Carbon and nitrogen peaks were visible in all four sample groups.

sed as a function of reaction times and aminosilane concentrations (Table 1). The coverslips in group D, which were soaked in 10% aminosilane solution for 12 h, exhibited the largest water contact angle of 86.2 ± 5.0°.

ATR-FTIR spectroscopy measurements

Based on the degree of absorption, infrared spectroscopy can help calculate the density of certain chemical groups on surfaces. A greater peak area (resulting from greater absorption) indicates a higher amino surface density. The infrared spectroscopy peak areas of amino groups exhibited a clear distribution with D > C > B > A (Table 1 and Fig. 1). Among all of the test samples, group D exhibited the highest peak, at approximately 0.00972, and the largest peak area, at approximately 1.15562.

X-ray photoelectron spectroscopy (XPS)

Carbon (binding energy, 281 eV) and nitrogen (binding energy, 395 eV) peaks were detected on all of the modified coverslips using XPS (Fig. 2). The presence of oxygen atom peaks might reflect oxidation or oxygen atom pollution in the free water of the aminosilane solution during the reaction process (Zelzer et al., 2008).

The surface amino densities

The amino densities on the surfaces of groups A, B, C, and D were 0.048 ± 0.006 μmol/mm^2, 0.128 ± 0.014 μmol/mm^2, 0.170 ± 0.010 μmol/mm^2, and 0.268 ± 0.013 μmol/mm^2 (n = 6), respectively. The density ratios (Table 1) calculated using the acid orange-7 assay were consistent with the data obtained using ATR-FTIR.

NSCs adhesion and migration on coverslips with various amino densities and PLL surfaces

The neurospheres on surfaces of the coverslips in D and PLL group exhibited the best biocompatibility and affinity (Fig. 3). For group A, after one day of culture, there were few attached neurospheres, and only a few single cells migrated out of the neurospheres. However, in the other groups (most notably for D and PLL group), more neurospheres attached and exhibited unclear round border; and a large number of cells migrated outwards from neurospheres and stretched out with long or short protrusions that were firmly attached to the material surface. On day five, morphological observation exhibited no significant difference. Each group exhibited two or more adjacent neurospheres with outwardly migrating cells that intertwined together as a mesh. Furthermore, the diameters of the neurospheres had decreased significantly compared to the first day; most of the cells had migrated outwards and had spread almost completely across the material surface.

Although differences in the attachment ratios of neurospheres were relatively small after 5 days culture (Fig. 4A), significant differences in the number of migratory cells surrounding the neurospheres were observed between the groups. PLL group had the most number of migrated cells, sequentially followed by group D, group C, group B, and group A ($p < 0.05$, Fig. 4B). And the increased amount of migrated cells depended on the amino densities increasing.

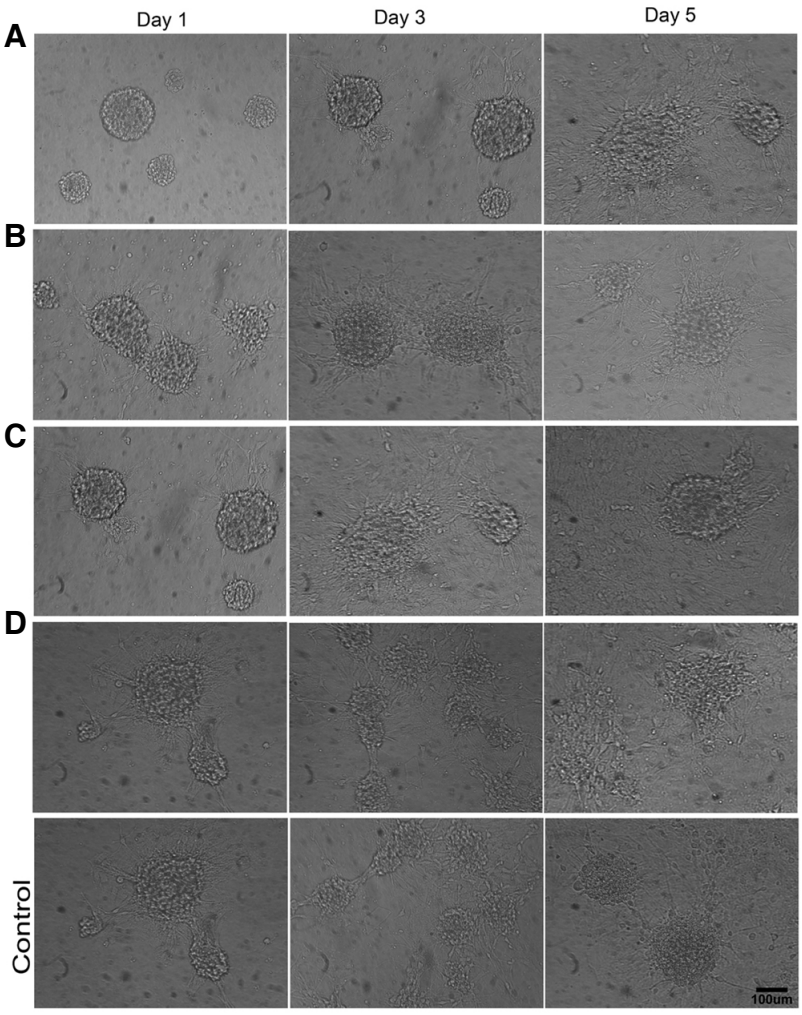

Fig. 3. The 200 neurospheres/cm^2 on the surfaces after one, three, and five days of culture under serum-free conditions. (A-D), amino modified surfaces with different densities; (Control), PLL coated surfaces. Scale bar = 100 μm.

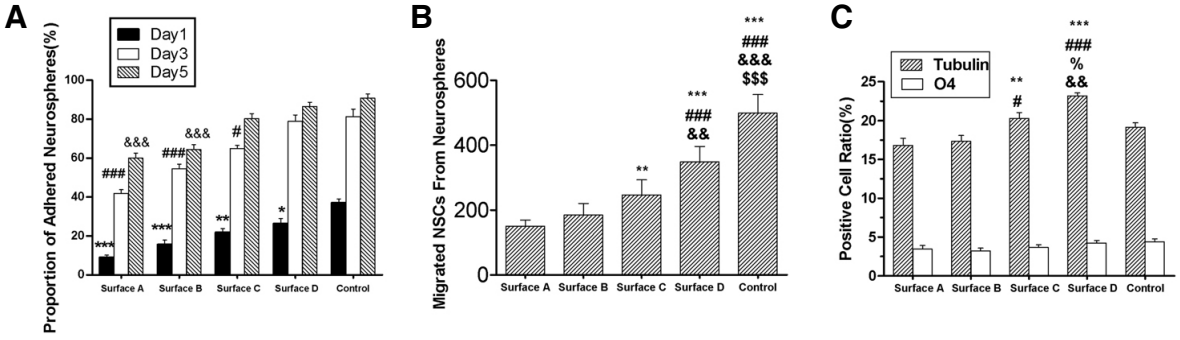

Fig. 4. Statistical charts in this study. (A) Neurosphere attachment ratios under serum-free conditions after one, three, and five days of culture. Three random fields were counted and displayed as the means ± standard error. Statistically significant one-way ANOVA results are indicated as follows: one symbol, $p < 0.05$; two symbols, $p < 0.01$; and three symbols, $p < 0.001$. *, compared with control group at the first day; #, compared with control group at the third day; &, compared with control group at the fifth day. (B) The number of cells migrated from neurospheres after five days of culture. Six random fields were counted and displayed as the means ± standard error. Statistically significant one-way ANOVA results are indicated as follows: one symbol, $p < 0.05$; two symbols, $p < 0.01$; and three symbols, $p < 0.001$. *, compared with group A; #, compared with group B; &, compared with group C; $, compared with group D. (C) Subtype cell counts after differentiation after seven days of culture. Six random fields were counted and are displayed as the means ± standard error. Statistically significant one-way ANOVA results are indicated as follows: one symbol, $p < 0.05$; two symbols, $p < 0.01$; and three symbols, $p < 0.001$. *, compared with group A; #, compared with group B; and &, compared with the percentage of group C; $, compared with control groups. There were no significant differences in the O_4-positive cell counts among all groups. (A-D), amino modified surfaces with different densities; (Control), PLL coated surfaces.

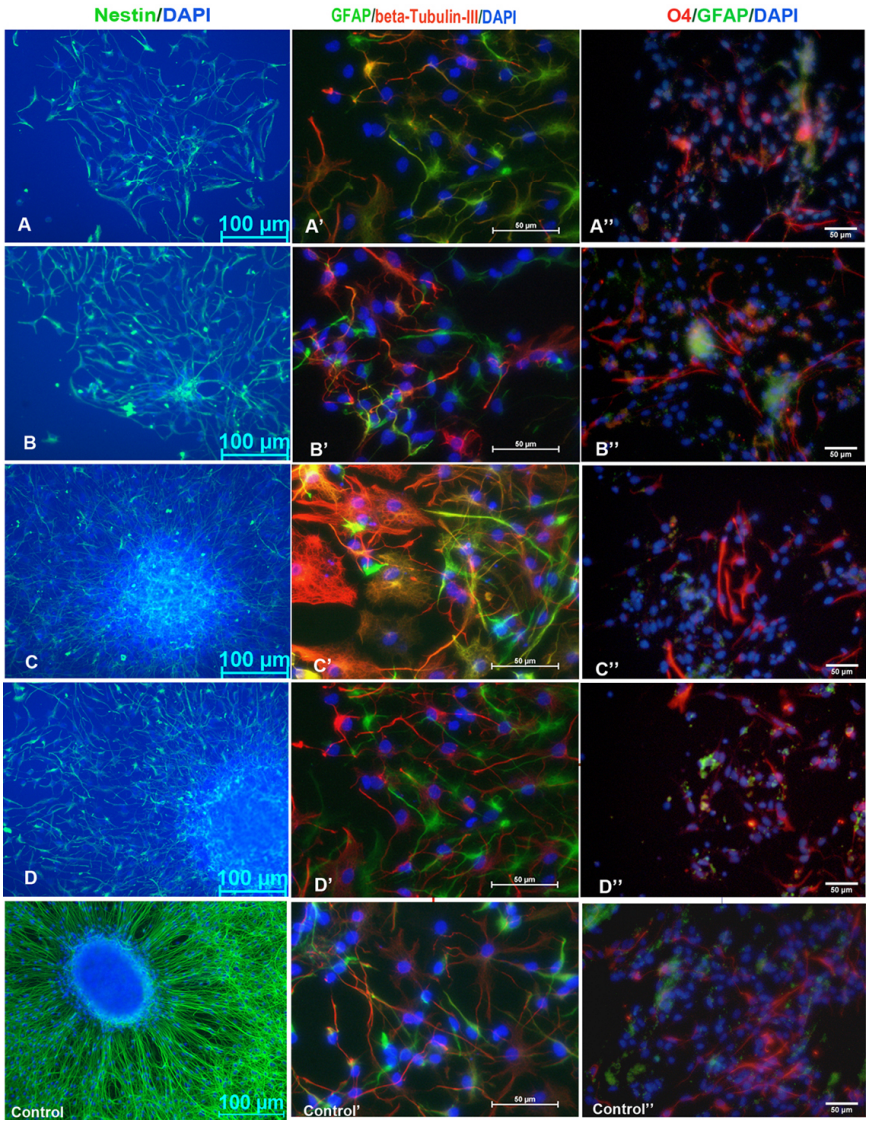

Fig. 5. Immunofluorescence staining of cell phenotypes cultured on the amino modified surfaces and PLL surfaces. Nestin immunofluo-rescence stained for NSCs after one day of culturing; GFAP, β-tubulin III and O_4 immunofluorescence double staining of NSCs differentiation showed astrocytes, neurons and oligodendrocytes after seven days of culturing. Blue indicates DAPI staining of nuclei. Scale bar (A-D), 100 μm; scale bar (A′B′C′D′ and A′′B′′C′′D′′), 50 μm. (A-D), amino modified surfaces with different densities; (Control), PLL coated surfaces.

Differentiation of neurosphere cells

At one and seven days after culture, the cell type-specific surface antigens Nestin, β-Tubulin III, GFAP, and O_4 were fluorescently labeled to identify differentiated states of NSCs (Fig. 5). Compared with the high-NH_2-density group D (23.17 ± 0.40%), neuronal differentiation ratios of group C was significantly lower ($p < 0.05$). The ratios of the lower -NH_2-density groups A and B were also significantly decreased ($p < 0.001$) (Fig. 4C). Al-though more cells migrated from neurospheres on PLL surface, the ratio of neuron differentiation on PLL surfaces lowered significantly than it on the highest amino density group ($p < 0.01$).

Ultrastructure of NSCs

The SEM analysis revealed that after five days of culture, each group contained neural stem cells with long protrusions attached to the amino-modified surface of the coverslips (as shown in Fig. 6A). After seven days of culture, TEM analysis of each group revealed the characteristic cytoskeletal structures and organelles of subtypes into which NSCs differentiate (Figs. 6B-6H).

DISCUSSION

NSCs differentiate into neurons, astrocytes, and oligodendrocytes (McKay, 1997). The broad application of NSCs has been demonstrated for the repair of nervous system injuries (Bible et al., 2009; Hwang et al., 2011; Johnson et al., 2010; Olson et al., 2009; Zhang et al., 2008). Although the effects of artificial, extracellular amino groups on the biological behavior of NSCs have been previously studied (Leipzig et al., 2011; Li et al., 2009), the impact of amino density on NSCs attachment, migration, and differentiation remains unknown. In the present study, coverslips with different amino densities were generated and used to characterize the effects amino density on rat NSCs behavior.

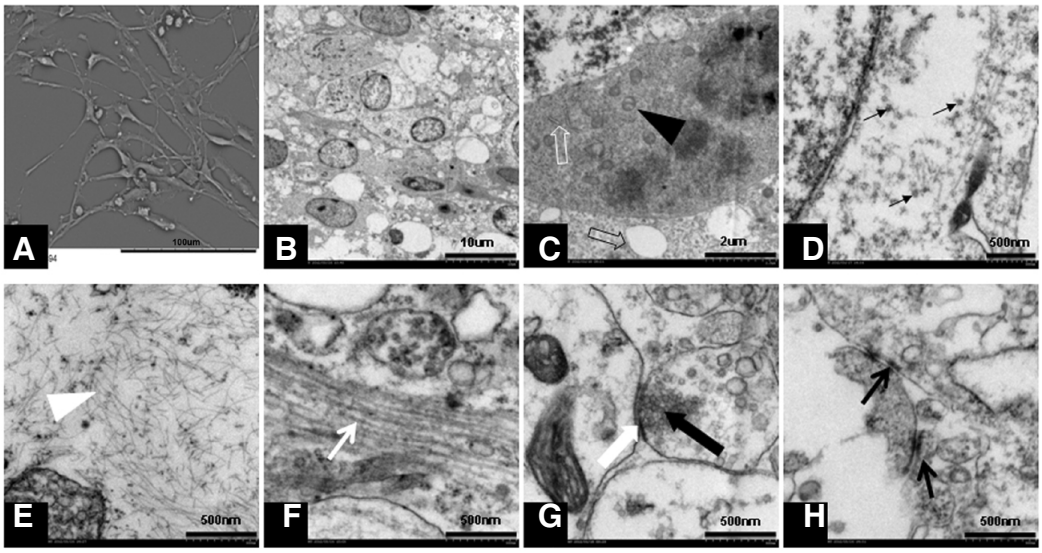

Fig. 6. Representative SEM and TEM images on amino modified and PLL coated surfaces. (A) A representative graph of all SEM analysises of NSCs after five days of culturing, stretched-out protrusions were visible. (B-H) representative graphs of TEM analysises on all tested surfaces. (B) Observation of neural stem cells after seven days of culturing: visible cell morphology showing a large nucleus, inverted nuclear-cytoplasm ratio, and small transparent cytoplasm; (C) the black solid arrow indicates mitochondria, the white hollow arrow indicates rough endoplasmic reticulum, and the black hollow arrow indicates expanded endoplasmic reticulum; (D) the black arrow indicates the white solid of the ribosome; (E) the white arrow indicates glial microfilaments; (F) the white arrow indicates neural microtubules; (G) the white solid arrow indicates synaptic cleft, the black solid arrow indicates neurotransmitter vesicles inside of the presynaptic membrane; and (H) the black arrows indicate the connections between cells. Scale bar in (A), 100 μm; scale bar in (B), 10 μm; scale bar in (C), 2 μm; scale bar in (D-G), and (H), 500 nm.

Adhesion

Previous studies have shown that changes in the density of carboxyl groups affect the surface charge and hydrophilicity of biological materials by regulating cell adhesion and guiding axonal growth (Li et al., 2005). Compared with other functional groups, the positive charge and good reactivity of amino provides significant advantages in promoting NSCs attachment (Engler et al., 2006; Faucheux et al., 2004; Hung et al., 2006; Neff et al., 1998; Ren et al., 2009; Wang et al., 2006). However, the specific interactions between cells and biological materials that regulate NSCs behavior remain unknown. In this study, we generated surfaces with different amino densities to determine whether functional group density or hydrophilicity can regulate NSCs attachment.

The hydrophilicity of biomaterial surfaces, which can induce a biological response (Lee et al., 2011), is typically determined by the WCA method. In this study, the chemical modification is actual a replacement of hydroxyl (OH) by polymethylene amino (CH2CH2NH2). The WCA measurements of groups A-D increased depending on amino density decreasing in our work. This WCA increasing may attribute to raising of the methylene amounts and better hydrophobicity of amino than hydroxyl. Generally, hydrophilicity favors cell attachment. However, despite being the least hydrophilic, group D had the highest number of attached NSCs suggesting that other surface features, such as surface charge and chemical density, play a more significant role in NSCs attachment.

Amino carries a positive charge and forms electrostatic interactions with negative charges on the cell surface. Thus, increasing the amino density on the surface might further improve the cell-surface material compatibility. Accordingly, the increase in NSCs attachment to surfaces with high amino densities was likely due to electrostatic attraction. Since cells surfaces are negatively charged, this electrochemical property is exclusive to the amino group. Indeed, Ren et al. (2009) showed that although hydroxyl displayed a smaller water contact angle, no improvement in NSCs attachment was observed. We suggest that the positive charge and higher reactivity of amino might help overcome losses in hydrophilicity, thereby mediating NSCs adhesion. Although higher amino densities were associated with higher number of attached cells in this study, amino compared unfavorably with polymer compound such as PLL in cells adhesion.

Migration

The amino density gradient affected NSCs migration in serum-free media. A higher amino density matrix might regulate the outward migration of cells in neurospheres. Hung et al. (2006) showed that there are no significant differences in the attachment and migration behaviors of cells on material surfaces with different active groups. However, these experiments were performed in serum-containing media. The culture environment used in the present study excluded interference from contaminating factors, such as serum and attachment proteins, thereby facilitating the characterization of the interactions between chemical groups and cells. Because the density of cultured neurospheres was similar for the different surface groups, the cell-to-cell contact forces were equivalent. Within modification, the cell-surface forces concomitantly increased with amino density and likely exceeded cell-to-cell forces, thus promoting the outward migration of NSCs. Compared with migrated cells on PLL surfaces, however, the benefit was not provided on amino surfaces.

Differentiation

Stem cell differentiation is regulated by a number of physical (Engler et al., 2006; Lee et al., 2011) and chemical (Ren et al., 2009) factors, particularly the chemical composition of the extracellular matrix (Hung et al., 2006). The results of the present study revealed that under conditioned of varying amino densities, NSCs differentiate into all the lineages we examined. Thus, the amino density does not affect the multi-lineage differentiation of NSCs. However, the neuronal differentiation ratio for the highest amino density (group D) is 23.19%, higher than it for the PLL group (19.17%). These data may indicate that higher amino density promotes neuronal differentiation of NSCs.

The SEM analysis showed that NSCs can attach and migrate on amino surface like on polymer substrate such as PLL (Cai et al., 2012). The TEM analysis revealed the presence of cytoskeletal structures, such as glial microfilaments, nerve microtubules, and non-symmetric synaptic structures (Merchan-Perez et al., 2009). Although we did not quantify the skeletal structures using electron microscopy, the presence of cytoskeletal structure suggested that amino can also promote the differentiation and maturation of NSCs as PLL can do (Fig. 6).

Another concern about the different response of NSCs to different amino density may attribute to amino internal geometry and three-dimensional space. In the chemical modification, longer reaction would generate thicker polymer layer or different three-dimensional space of amino groups. Even minor variations in the internal geometry (Soman et al., 2012) and three-dimensional space (Han et al., 2012; Rampichova et al., 2013) can impact cell survival, growth, and fate choice.

In the present study, we demonstrated that the density of amino groups on cell culture materials affects the behavior of NSCs and is therefore an important factor for tissue engineering technology. The polymerization of amino acids with more active amino side chains or proteins with more active amino functional sites could increase NSCs adhesion, migration, and neuronal differentiation. Thus, both the type and density of active chemical groups should be considered in surface modification studies of biological materials.

Note: Supplementary information is available on the Molecules and Cells website (www.molcells.org).

REFERENCES

Ananthanarayanan, B., Little, L., Schaffer, D.V., Healy, K.E., and Tirrell, M. (2010). Neural stem cell adhesion and proliferation on phospholipid bilayers functionalized with RGD peptides. Biomaterials *31*, 8706-8715.

Badoyannis, H.C., Sharma, S.C., and Sabban, E.L. (1991). The differential effects of cell density and NGF on the expression of tyrosine hydroxylase and dopamine beta-hydroxylase in PC12 cells. Brain Res. Mol. Brain Res. *11*, 79-87.

Bible, E., Chau, D.Y., Alexander, M.R., Price, J., Shakesheff, K.M., and Modo, M. (2009). The support of neural stem cells transplanted into stroke-induced brain cavities by PLGA particles. Biomaterials *30*, 2985-2994.

Brewer, G.J., and Torricelli, J.R. (2007). Isolation and culture of adult neurons and neurospheres. Nat. Protocols *2*, 1490-1498.

Cai, L., Lu, J., Sheen, V., and Wang, S. (2012). Optimal poly(L-lysine) grafting density in hydrogels for promoting neural progenitor cell functions. Biomacromolecules *13*, 1663-1674.

Cook, A.D., Pajvani, U.B., Hrkach, J.S., Cannizzaro, S.M., and Langer, R. (1997). Colorimetric analysis of surface reactive amino groups on poly(lactic acid-co-lysine):poly(lactic acid) blends. Biomaterials *18*, 1417-1424.

Engler, A.J., Sen, S., Sweeney, H.L., and Discher, D.E. (2006). Matrix elasticity directs stem cell lineage specification. Cell *126*, 677-689.

Faucheux, N., Schweiss, R., Lutzow, K., Werner, C., and Groth, T. (2004). Self-assembled monolayers with different terminating groups as model substrates for cell adhesion studies. Biomaterials *25*, 2721-2730.

Han, S., Yang, K., Shin, Y., Lee, J.S., Kamm, R.D., Chung, S., and Cho, S.W. (2012). Three-dimensional extracellular matrix-mediated neural stem cell differentiation in a microfluidic device. Lab. Chip. *12*, 2305-2308.

Ho, M., Yu, D., Davidsion, M.C., and Silva, G.A. (2006). Comparison of standard surface chemistries for culturing mesenchymal stem cells prior to neural differentiation. Biomaterials *27*, 4333-4339.

Horwitz, J.A., Shum, K.M., Bodle, J.C., Deng, M., Chu, C.C., and Reinhart-King, C.A. (2010). Biological performance of biodegradable amino acid-based poly(ester amide)s: Endothelial cell adhesion and inflammation *in vitro*. J. Biomed. Mater. Res. A *95*, 371-380.

Hu, S.G., Jou, C.H., and Yang, M.C. (2002). Surface grafting of polyester fiber with chitosan and the antibacterial activity of pathogenic bacteria. J. Appl. Polym. Sci. *86*, 2977-2983.

Hung, C.H., Lin, Y.L., and Young, T.H. (2006). The effect of chitosan and PVDF substrates on the behavior of embryonic rat cerebral cortical stem cells. Biomaterials *27*, 4461-4469.

Hwang, D.H., Kim, H.M., Kang, Y.M., Joo, I.S., Cho, C.S., Yoon, B.W., Kim, S.U., and Kim, B.G. (2011). Combination of multifaceted strategies to maximize the therapeutic benefits of neural stem cell transplantation for spinal cord repair. Cell Transplant. *20*, 1361-1379.

Johnson, P.J., Tatara, A., Shiu, A., and Sakiyama-Elbert, S.E. (2010). Controlled release of neurotrophin-3 and platelet-derived growth factor from fibrin scaffolds containing neural progenitor cells enhances survival and differentiation into neurons in a subacute model of SCI. Cell Transplant. *19*, 89-101.

Keselowsky, B.G., Collard, D.M., and Garcia, A.J. (2004). Surface chemistry modulates focal adhesion composition and signaling through changes in integrin binding. Biomaterials *25*, 5947-5954.

Lee, J.H., Jung, H.W., Kang, I.K., and Lee, H.B. (1994). Cell behaviour on polymer surfaces with different functional groups. Biomaterials *15*, 705-711.

Lee, S., Kim, J., Park, T.J., Shin, Y., Lee, S.Y., Han, Y.M., Kang, S., and Park, H.S. (2011). The effects of the physical properties of culture substrates on the growth and differentiation of human embryonic stem cells. Biomaterials *32*, 8816-8829.

Leipzig, N.D., Wylie, R.G., Kim, H., and Shoichet, M.S. (2011). Differentiation of neural stem cells in three-dimensional growth factor-immobilized chitosan hydrogel scaffolds. Biomaterials *32*, 57-64.

Li, B., Ma, Y., Wang, S., and Moran, P.M. (2005). Influence of carboxyl group density on neuron cell attachment and differentiation behavior: gradient-guided neurite outgrowth. Biomaterials *26*, 4956-4963.

Li, X., Yang, Z., and Zhang, A. (2009). The effect of neurotrophin-3/chitosan carriers on the proliferation and differentiation of neural stem cells. Biomaterials *30*, 4978-4985.

McKay, R. (1997). Stem cells in the central nervous system. Science *276*, 66-71.

Merchan-Perez, A., Rodriguez, J.R., Alonso-Nanclares, L., Schertel, A., and Defelipe, J. (2009). Counting synapses using FIB/SEM microscopy: a true revolution for ultrastructural volume reconstruction. Front. Neuroanat. *3*, 18.

Neff, J.A., Caldwell, K.D., and Tresco, P.A. (1998). A novel method for surface modification to promote cell attachment to hydrophobic substrates. J. Biomed. Mater. Res. *40*, 511-519.

Olson, H.E., Rooney, G.E., Gross, L., Nesbitt, J.J., Galvin, K.E., Knight, A., Chen, B., Yaszemski, M.J., and Windebank, A.J. (2009). Neural stem cell- and Schwann cell-loaded biodegradable polymer scaffolds support axonal regeneration in the transected spinal cord. Tissue Eng. Part A *15*, 1797-1805.

Rampichova, M., Chvojka, J., Buzgo, M., Prosecka, E., Mikes, P., Vyslouzilova, L., Tvrdik, D., Kochova, P., Gregor, T., Lukas, D., et al. (2013). Elastic three-dimensional poly (epsilon-caprolactone) nanofibre scaffold enhances migration, proliferation and osteogenic differentiation of mesenchymal stem cells. Cell Prolif. *46*, 23-37.

Ren, Y.J., Zhang, H., Huang, H., Wang, X.M., Zhou, Z.Y., Cui, F.Z., and An, Y.H. (2009). *In vitro* behavior of neural stem cells in

response to different chemical functional groups. Biomaterials *30*, 1036-1044.
Soman, P., Tobe, B.T., Lee, J.W., Winquist, A.A., Singec, I., Vecchio, K.S., Snyder, E.Y., and Chen, S. (2012). Three-dimensional scaffolding to investigate neuronal derivatives of human embryonic stem cells. Biomed. Microdevices *14*, 829-838.
Symons, J.R., LeVea, C.M., and Mooney, R.A. (2002). Expression of the leucocyte common antigen-related (LAR) tyrosine phosphatase is regulated by cell density through functional E-cadherin complexes. Biochem. J. *365*, 513-519.
Teng, X., Ren, J., and Gu, S. (2007). Preparation and characterization of porous PDLLA/HA composite foams by supercritical carbon dioxide technology. J. Biomed. Mater. Res. B Appl. Biomater. *81*, 185-193.
Vasita, R., Shanmugam, I.K., and Katt, D.S. (2008). Improved biomaterials for tissue engineering applications: surface modification of polymers. Curr. Top. Med. Chem. *8*, 341-353.
Wang, J.H., Hung, C.H., and Young, T.H. (2006). Proliferation and differentiation of neural stem cells on lysine-alanine sequential polymer substrates. Biomaterials *27*, 3441-3450.
Zelzer, M., Majani, R., Bradley, J.W., Rose, F.R., Davies, M.C., and Alexander, M.R. (2008). Investigation of cell-surface interactions using chemical gradients formed from plasma polymers. Biomaterials *29*, 172-184.
Zhang, H., Wei, Y.T., Tsang, K.S., Sun, C.R., Li, J., Huang, H., Cui, F.Z., and An, Y.H. (2008). Implantation of neural stem cells embedded in hyaluronic acid and collagen composite conduit promotes regeneration in a rabbit facial nerve injury model. J. Translat. Med. *6*, 67.